Effects of quantum interference between radiative and dielectronic recombination on photorecombination cross-section profiles for the He-like ions Ar^{16+} and Fe^{24+}

Ehud Behar
Physics Department, Technion, Haifa 32000, Israel

Verne L. Jacobs
Center for Computational Materials Science, Code 6390.2, Materials Science and Technology Division, Naval Research Laboratory, Washington, DC 20375-5345, USA

Joseph Oreg and Avi Bar-Shalom
Nuclear Research Center-Negev, P.O. Box 9001, 84190 Beer-Sheva, Israel

Stanley L. Haan
Department of Physics and Astronomy, Calvin College, Grand Rapids, Michigan 49546, USA
(Received 2 May 2003; revised manuscript received 20 September 2003; published 12 February 2004)

Total cross sections for electron-ion photorecombination (PR) processes are calculated using a projection-operator and resolvent-operator approach. This approach provides a unified quantum-mechanical description of the combined electron-ion PR process, including radiative and dielectronic recombination as coherent, interfering components. An especially adapted version of the Hebrew-University Lawrence-Livermore Atomic Code HULLAC is developed and employed for the calculations. In particular, PR cross sections for He-like argon and iron ions are calculated for incident-electron energies in the vicinity of the $1s2l2l'$ and $1s2l3l'$ doubly-excited, autoionizing levels of the Li-like ions. Significant effects of quantum interference between radiative and dielectronic recombination, in the form of asymmetric PR cross-section profiles, are predicted, especially for weak transitions. The general behavior of the interference effect, as a function of the ion charge q and as a function of the principal quantum number n' of the outer electron in the autoionizing state, is investigated using a hydrogenic-scaling analysis. It is found that the degree of asymmetry in the PR cross-section profile can be substantial for close-to-neutral ions and also for very highly-charged ions. In the intermediate-charge regime, on the other hand, the asymmetry is anticipated to be less prominent. The dependence of the quantum-interference effect on n' is predicted to be much weaker.

DOI: 10.1103/PhysRevA.69.022704 PACS number(s): 32.80.Dz, 34.80.Kw, 32.70.Jz

I. INTRODUCTION

The photorecombination (PR) process of a multiply charged ion with a free electron, involving radiative emission, is traditionally described in terms of two distinct recombination mechanisms. The first is nonresonant or direct radiative recombination (RR), which is the inverse of the ordinary photoionization process, and the second corresponds to the first-order diagrammatic correction, namely the two-step, resonant dielectronic recombination (DR) process. These two recombination mechanisms are usually treated as independent processes. It has been recognized, however, that the traditional description of RR and DR, as two independent, noninterfering processes, is not strictly permissible within the framework of a rigorous quantum-mechanical theory [1–4]. For a fundamental quantum-mechanical description of the entire, combined PR process, RR and DR must be treated as coherent, interfering components of a single electromagnetic transition occurring between the relevant initial and final atomic states. The need for a corresponding treatment of the resonant and nonresonant (time-reversed) photoionization mechanisms has been firmly established. Several theoretical investigations have been carried out (e.g., [5–9]) in pursuit of prominent manifestations of the quantum-mechanical interference between RR and DR. Asymmetrical PR cross-section profiles, which are characteristic spectral signatures of a prominent quantum-interference effect, have been observed by Knapp *et al.* [10] for the PR of very highly-charged uranium ions in an electron-beam ion trap (EBIT). In a recent storage-ring experiment, broad, asymmetrical PR profiles have been detected for Sc^{3+} [11]. In that investigation, the observed profiles have been attributed not only to the quantum interference between RR and DR, but also to the interaction among neighboring, overlapping DR resonances. Except for these special cases, the customary independent-processes and isolated-resonance approximation has been found to be very successful in describing the overwhelming majority of PR cross-section experiments. Pindzola *et al.* [12] have presented convincing physical explanations for the success of the standard approximation in the vast majority of cases. Nevertheless, it is worthwhile to persist in the search for exceptional transitions for which the fundamental quantum-mechanical interference phenomenon would be revealed.

Efforts to provide a unified quantum-mechanical description of RR and DR have primarily involved two major, alternative approaches. The first major approach is based on a radiative modification of the close-coupling equations [13,14]. This inherently nonperturbative approach can be applied using existing close-coupling or *R*-matrix codes [15],

and overlapping resonances can be naturally treated. However, only a relatively small, and in many cases insufficient [16], number of coupled channels can be taken into account in practical calculations. Furthermore, in order to resolve adequately the narrow PR resonances, it is often necessary to perform the calculations for a very large number of energy points or to use the results of other calculations as a guide [17]. An additional difficulty in the radiatively modified close-coupling approach is the absence of a transparent procedure for extending this approach to allow for the incorporation of collisional decoherence and relaxation processes involving the autoionizing states, which can become important at sufficiently high densities.

In the present investigation, we employ an alternative approach that is based on projection-operator and resolvent-operator methods [2,4,18]. By means of this alternative approach, the transition operator describing the entire electron-ion PR process is naturally expressed as a sum of a direct nonresonant RR contribution and an indirect resonant term corresponding to DR. This approach [18] provides a general nonperturbative procedure for obtaining the required matrix elements of the transition operator for model systems featuring a limited number of discrete, autoionizing states and single-electron and single-photon continuum channels. In our calculations, we evaluate the leading term in a perturbation-theory expansion for the relevant matrix elements of the PR transition operator. This leading contribution has been derived [18] and evaluated in an investigation by Zimmermann *et al.* [19]. Recently, we have adopted this lowest-order approximation to obtain a convenient analytical formula for a parameter that meaningfully reflects the degree of asymmetry in the energy profile of the PR cross section [9]. This analytical formula was then evaluated to identify PR transitions of He-like Ar and Fe ions for which the effects of quantum interference may be observable. It is important to note that the present ordinary Hilbert-space approach is appropriate only for the low-density regime, for which it is permissible to neglect electron-ion collisional processes that involve ions in autoionizing states. For higher densities, collisional decoherence and relaxation processes should be incorporated. A Liouville-space (reduced-density-operator) generalization of the ordinary Hilbert-space projection-operator and resolvent-operator approach has been presented by Jacobs *et al.* [20]. This generalization provides the fundamental framework for the incorporation of both collisional and radiative decoherence and relaxation processes.

In this paper, we present the results of calculations for the entire set of PR transitions involving the $1s2l2l'$ and $1s2l3l'$ doubly-excited, autoionizing states of He-like Ar and Fe ions. The effect of the quantum interference between RR and DR on the $1s2l2l'$ satellite-line intensities was first investigated for the He-like Ar ion by Jacobs *et al.* [21]. In that investigation, the main emphasis was on the total (energy-integrated) intensities of the dielectronic-satellite lines. In the present investigation, the primary focus is on the detailed energy profiles of the individual PR cross sections. Moreover, we have extended the scope of the first calculations [21] to include the He-like Fe^{24+} ion and also to treat transitions involving the higher lying $1s2l3l'$ doubly-excited, autoionizing states. The results obtained for the Fe $1s2l2l'$ resonances are compared to the level-specific DR cross-section parameters that have been measured using EBIT by Beiersdorfer *et al.* [22].

The remainder of the paper is organized as follows: In Sec. II, a brief review of the projection-operator and resolvent-operator approach is provided. In Sec. III, we give the explicit expressions for the various components of the PR cross section, which we have obtained from the evaluation of the lowest-order contribution in the perturbation-theory expansion. In Sec. IV, our detailed numerical results are presented. Finally, in Sec. V the expression for the profile asymmetry parameter, which we have introduced [9], is employed in a hydrogenic-scaling analysis of the quantum-mechanical interference effect. Our objective is to provide guidance for future experimental observations of the spectral signature due to the quantum interference between RR and DR.

II. THE PROJECTION-OPERATOR AND RESOLVENT-OPERATOR APPROACH

The ordinary Hilbert-space projection-operator and resolvent-operator formulation [18] provides a fundamental foundation for a unified quantum-mechanical description of radiative and dielectronic recombination in the absence of collisional and radiative decoherence and relaxation processes. Accordingly, this description is expected to be rigorously valid at sufficiently low plasma densities and radiation-field intensities.

The combined system, consisting of the recombining ion, the incident electron, and the radiation field, can be described in terms of the total Hamiltonian operator $H=H^0+V$, where H^0 is the sum of the unperturbed Hamiltonian operators for the non-interacting systems. The interaction operator V includes, on an equal footing, both the electron-electron electrostatic (Coulombic) interaction and the interaction of the atomic system with the quantized electromagnetic field. These interactions are responsible for the autoionization and spontaneous radiative-emission processes, respectively. The unperturbed eigenstates relevant to the PR process may be separated into three distinct classes of states. Single-electron continuum states will be represented by $|i\vec{p}\rangle$, where i denotes the initial state of the recombining ion (with charge q) and $\vec{p}$ is the linear momentum of the incident electron. Discrete, doubly-excited, autoionizing states of the recombined ion (with charge $q-1$) will be represented by $|d\rangle$. Finally, single-photon continuum states will be represented by $|f\vec{k}\rangle$, where f denotes the final state of the recombined ion (with charge $q-1$) and $\vec{k}$ is the linear momentum of the emitted photon. The various energies must satisfy the condition expressing conservation of total energy E:

$$E=E_i+\varepsilon=E_d=E_f+\hbar\omega. \tag{1}$$

Here, E_i is the energy of the recombining ion in the initial state i, E_f is the energy of the recombined atomic system in the final state f, and E_d is the energy of the doubly-excited,

autoionizing atomic state $|d\rangle$. The energies of the incident electron and emitted photon are denoted by ε and $\hbar\omega$, respectively.

The transition operator $T(z)$ can be defined, as a function of the complex variable z, by

$$T(z)=V+VG(z)V. \tag{2}$$

The resolvent (or Green's) operator $G(z)=(z-H)^{-1}$ corresponds to the full Hamiltonian operator H. The total PR cross section $\sigma_{if}^{PR}(\varepsilon)$, for the composite radiative-emission process leading to the transition $i\rightarrow f$, can be expressed in the form

$$\sigma_{if}^{PR}(\varepsilon)=\lim_{\eta\downarrow 0}\left(\frac{2\pi}{\hbar}\right)\left(\frac{1}{4\pi}\right) \times\frac{\int d\Omega_{\vec{p}}\int d\Omega_{\vec{k}}|\langle f\vec{k}|T(E+i\eta)|i\vec{p}\rangle|^2}{F(\vec{p})}\rho(\hbar\omega), \tag{3}$$

where $\rho(\hbar\omega)$ is the density of final states per unit energy and per solid angle intervals and $F(\vec{p})$ is the incoming electron flux. This cross section involves an average over all incident-electron directions $\Omega_{\vec{p}}$ and an integration over all outgoing-photon directions $\Omega_{\vec{k}}$. In the familiar Fermi golden rule result obtained in lowest-order perturbation theory, the full transition operator $T(z)$ would be replaced by the interaction operator V alone.

Employing projection-operator techniques [18], the transition operator $T(z)$ can be rearranged to provide a natural separation into direct, nonresonant and indirect, resonant components. Consequently, the total PR cross section [Eq. (3)], describing the transition $i\rightarrow f$ for incident-electron energies ε in the vicinity of a discrete autoionizing level d, can be unambiguously expressed as a sum of three contributions:

$$\sigma_{if}^{PR}(\varepsilon)=\sigma_{if}^{RR}(\varepsilon)+\sigma_{idf}^{DR}(\varepsilon)+\sigma_{idf}^{int}(\varepsilon). \tag{4}$$

The three individual contributions correspond to the RR cross section, the DR cross section, and the product term representing the interference (denoted by *int*) between the RR and the DR transition amplitudes.

A nonperturbative procedure has been developed [18] for the explicit evaluation of the desired matrix elements of the projected transition operator describing the entire PR process. For the most general case, including multiple electron and multiple photon continua, the implementation of this procedure involves the calculation and inversion of matrices than can become very large for complex atomic systems. In order to circumvent this difficulty, an alternative perturbation-theory-expansion procedure [18] can be employed. The lowest-order contribution in this perturbation-theory expansion has been adopted in earlier calculations [19,9] and is now utilized for the more extensive calculations reported in this paper. In this lowest-order approximation, the expressions for the RR and DR cross sections are found to be identical to the well-known results obtained in the familiar independent-processes and isolated-resonance approximation. However, even in this lowest-order approximation of the unified description, the additional quantum-mechanical interference term is predicted.

III. EXPRESSIONS FOR THE COMPONENTS OF THE PR CROSS SECTION

In order to compute the PR cross sections using existing atomic structure and collision codes, such as HULLAC [23], the various atomic states must be more fully specified in the appropriate angular-momentum representation. We shall neglect hyperfine structure and specify the atomic eigenstates i, d, and f in terms of the total electronic angular-momentum quantum numbers J_i, J_d, and J_f, respectively. We specify the state of the incident electron using the quantum number $\kappa=(l-j)(2j+1)$, corresponding to the single-electron total and orbital angular-momentum quantum numbers j and l, respectively. Accordingly, the unperturbed eigenstates of the combined system (composed of the initial atomic system, the incident electron, and the emitted photon) can be more fully specified as follows:

$$|i\vec{p}\rangle=|\gamma_i J_i,\vec{p}\,\kappa;J\rangle,$$
$$|d\rangle=|\gamma_d J_d\rangle, \tag{5}$$
$$|f\vec{k}\rangle=|\gamma_f J_f,\vec{k}\rangle,$$

where the symbols labeled by γ represent sets of additional atomic quantum numbers not indicated explicitly, including the principal quantum numbers and the magnetic quantum numbers. The photon polarization is also not specified explicitly but may be included in γ_f. Summations and averages over the magnetic and photon-polarization quantum numbers are not explicitly indicated but are taken into account. Invoking conservation of the total electronic angular momentum in the radiationless transitions connecting the autoionizing resonance states and the corresponding nonresonant electron-continuum states, we obtain the requirement that $J=J_d$. In the following analysis, we will specify the electron-continuum states in terms of the electron energy ε and use the energy-normalization convention.

In the electric-dipole approximation, the lowest-order contribution to the RR cross section can be reduced to the familiar result:

$$\sigma_{if}^{RR}(\varepsilon)=\frac{1}{2(2J_i+1)}\frac{4\pi^2\hbar^2\omega^3}{3c^3p^2} \times\sum_{\kappa}\sum_{J}|\langle\gamma_f J_f\|\vec{D}\|\gamma_i J_i,\varepsilon\kappa;J\rangle|^2, \tag{6}$$

which is expressed in terms of reduced matrix elements of the many-electron electric-dipole moment operator $\vec{D}=e\Sigma\vec{r}_j$ between the discrete and (energy-normalized) continuum electronic states.

The transition amplitude for DR is most easily evaluated after introducing the pole approximation for the resolvent

operators [18]. In the lowest-order perturbation-theory evaluation, we recover the familiar expression for the DR cross section:

$$\sigma_{idf}^{DR}(\varepsilon)=\frac{(2\pi\hbar)^3}{8\pi m\varepsilon}\frac{(2J_d+1)}{2(2J_i+1)}A_{di}^{a}L_d(\varepsilon)B_{df}^{D}. \tag{7}$$

The rate for autoionization from the resonance state d to the nonresonant electron-continuum state i and is given by

$$A_{di}^{a}=\frac{2\pi}{\hbar}\frac{1}{(2J_d+1)}\sum_{\kappa}|\langle\gamma_i J_i,\varepsilon\kappa;J\|H_{es}\|\gamma_d J_d\rangle|^2\delta_{E_d,E_i+\varepsilon}. \tag{8}$$

H_{es} is the familiar electron-electron electrostatic-interaction operator $e\Sigma(r_{kl})^{-1}$. The energy-normalized Lorentzian line-shape function is given by

$$L_d(\varepsilon)=\frac{\Gamma(d)/2\pi}{(E_i+\varepsilon-E_d)^2+\left(\frac{\Gamma(d)}{2}\right)^2}. \tag{9}$$

The total (natural) width of the doubly-excited, autoionizing level d, in the absence of environmental interactions, is given by

$$\Gamma(d)=\hbar\left(\sum_f A_{df}+\sum_i A_{di}^{a}\right). \tag{10}$$

The Einstein A coefficient for spontaneous radiative decay from the state d to the state f can be written as follows:

$$A_{df}=\frac{4e^2\omega^3}{3\hbar c^3}\frac{1}{(2J_d+1)}|\langle\gamma_f J_f\|\vec{D}\|\gamma_d J_d\rangle|^2\delta_{E_d,E_f+\hbar\omega}. \tag{11}$$

The quantity

$$B_{df}^{D}=\frac{\hbar A_{df}}{\Gamma(d)} \tag{12}$$

is the branching ratio corresponding to the probability for the spontaneous radiative transition $d\rightarrow f$.

In electron beam experiments, such as those performed with EBIT, the ideal measurement would yield the PR cross section, as a function of the incident-electron energy ε. However, the natural width $\Gamma(d)$ of the DR resonance profile can be about two orders of magnitude smaller than the typical EBIT electron-energy resolution of $\sim$50 eV. Consequently, one introduces a resonance-transition strength S_{idf}, which is obtained from the PR cross section by integration over incident-electron energies covering the immediate region of the resonance level d:

$$S_{idf}=\int\sigma_{if}^{PR}(\varepsilon)d\varepsilon=\frac{(2\pi\hbar)^3}{8\pi m(E_d-E_i)}\frac{(2J_d+1)}{2(2J_i+1)}A_{di}^{a}B_{df}^{D}. \tag{13}$$

On the right-hand side of Eq. (13), the resonance-transition strength is evaluated using the lowest-order DR cross section. The lowest-order interference cross section, which is found below to be an antisymmetric function of energy near the resonance level, gives a vanishing contribution. In addition, the contribution of the slowly varying nonresonant RR cross section has been omitted in the lowest-order evaluation of the resonance-transition strength. The resonance-transition strength defined by Eq. (13) more nearly corresponds to the experimentally accessible quantity, especially in the limit of a very narrow resonance line shape.

In terms of the familiar (lowest-order) autoionization and radiative-decay rates, and of the (lowest-order) DR cross section, the (lowest-order) interference contribution to the PR cross section can be expressed in the simplified form [19]:

$$\sigma_{idf}^{int}(\varepsilon)=\frac{4}{\hbar A_{di}^{a}}\left[(E_i+\varepsilon-E_d)\left(\frac{1}{Q_{idf}}\right)\right]\sigma_{idf}^{DR}(\varepsilon), \tag{14}$$

where the multichannel Fano line-profile parameter Q_{idf} is defined by

$$\frac{1}{Q_{idf}}=\frac{\pi}{(2J_d+1)^{1/2}}\times\frac{\sum_{\kappa}\langle\gamma_f J_f\|\vec{D}\|\gamma_i J_i,\varepsilon\kappa;J\rangle\langle\gamma_i J_i,\varepsilon\kappa;J\|H_{es}\|\gamma_d J_d\rangle}{\langle\gamma_f J_f\|\vec{D}\|\gamma_d J_d\rangle}. \tag{15}$$

Equation (15) can be compared with Eq. (86) in the earlier investigation of the quantum interference [4]. They are found to be in agreement to first order in the small parameter $1/Q_{idf}$, since in this approximation the continuum-continuum coupling parameter introduced in the earlier investigation can be set to unity. Zimmermann *et al.* [19] have extended this analysis for higher-order electromagnetic-multiple transitions, for which $1/Q_{idf}$ can have an imaginary part, in addition to the real part given by Eq. (15). It can be seen from Eq. (14) that the electron-energy dependence of the (lowest-order) quantum-interference contribution to the total PR cross section, for energies in the vicinity of a DR resonance, is a consequence of the product of a linear function of ε, which changes sign at the position of the resonance energy $\varepsilon=E_d-E_i$, and the symmetric Lorentzian-profile function associated with the unperturbed (lowest-order) DR cross section. Accordingly, this energy dependence corresponds to an asymmetric (Fano-type) energy profile, which has been observed in the EBIT experiment by Knapp *et al.* [10]. After computing the transition amplitudes and rates that appear in Eqs. (6), (7), and (14), one can evaluate all lowest-order contributions to the total PR cross section, taking into account both the RR and DR mechanisms together with their quantum-mechanical interference.

In our earlier calculations [9], we introduced a parameter that reflects the degree of the asymmetry in the PR cross section. This parameter was defined by evaluating the (lowest-order) DR and interference components of the PR cross section at the off-resonance electron energies $\varepsilon_{\pm 1/2}$,

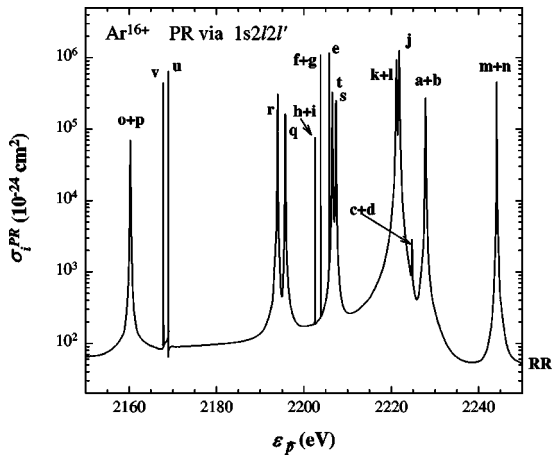

FIG. 1. Total cross section for PR of He-like Ar^{16+} for incident-electron energies in the vicinity of the Li-like $1s2l2l'$ doubly-excited, autoionizing complex, as a function of the incident-electron energy. The continuum contribution to the total PR cross section corresponds to the unperturbed RR component.

$$\varepsilon_{\pm 1/2} = E_d - E_i \pm \frac{\Gamma(d)}{2}. \tag{16}$$

At these two off-resonance electron energies, the (lowest-order) quantum-interference contribution has an extremum [a maximum or minimum, depending on the sign in front of $\Gamma(d)$ in Eq. (16)], and the (lowest-order) DR cross section attains one half of its maximum value. At either one of these electron energies, the absolute value of the (lowest-order) ratio of the interference contribution and the DR cross section is given by the relationship

$$R^{int} = \left| \frac{\sigma_{idf}^{int}(\varepsilon_{\pm 1/2})}{\sigma_{idf}^{DR}(\varepsilon_{\pm 1/2})} \right| = \frac{4}{\hbar A_{di}^{a}} \frac{\Gamma(d)}{2} \left| \frac{1}{Q_{idf}} \right|. \tag{17}$$

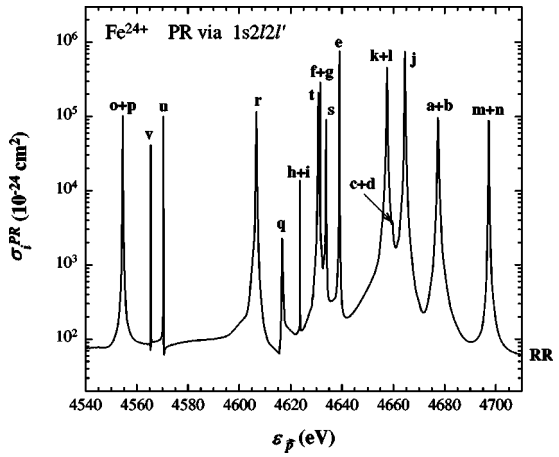

FIG. 2. Total cross section for PR of He-like Fe^{24+} for incident-electron energies in the vicinity of the Li-like $1s2l2l'$ doubly-excited, autoionizing complex, as a function of the incident-electron energy. The continuum contribution to the total PR cross section corresponds to the unperturbed RR component.

TABLE I. Resonances in the cross section for DR of He-like Ar^{16+} through the Li-like $1s2l2l'$ doubly-excited, autoionizing complex. The DR resonance transitions are labeled using the notation introduced by Gabriel [24]. E_{id} is the resonance energy. S_{idf} is the lowest-order resonance-transition strength, defined as an integration over the resonance profile by Eq. (13), for which the interference contribution vanishes and the RR contribution has been omitted. Numbers in square brackets indicate powers of ten.

Transition	E_{id} (eV)	S_{idf} (eV cm^2)
o	2160.3	6.06[−21]
p	2160.3	3.77[−21]
v	2167.8	6.54[−23]
u	2168.9	2.39[−22]
r	2194.0	3.09[−20]
q	2195.7	1.67[−20]
h	2202.5	1.00[−24]
i	2202.5	2.10[−23]
f	2203.9	5.20[−22]
g	2203.9	7.20[−24]
e	2205.8	4.90[−21]
t	2206.5	3.68[−20]
s	2207.3	2.70[−20]
k	2221.2	1.83[−19]
l	2221.2	5.07[−24]
j	2221.8	2.50[−19]
c	2224.8	9.46[−23]
d	2224.8	2.37[−22]
a	2227.8	3.72[−20]
b	2227.8	2.87[−21]
m	2244.1	2.68[−20]
n	2244.1	5.88[−20]

For a larger value of this ratio, a more asymmetric profile is predicted for the total PR cross section.

IV. CALCULATIONS FOR He-LIKE Ar AND Fe IONS

In this section, we report the results of detailed (level-by-level) *ab initio* computations for the electron-ion photorecombination cross sections of ground-state He-like argon ($Z=18$) and iron ($Z=26$) ions, for incident-electron energies in the vicinity of the $1s2l2l'$ and $1s2l3l'$ autoionizing-configuration complexes of the corresponding Li-like ions. These computations have been based on the theoretical approach described in the preceding sections. Configuration mixing within each complex has been fully included. The composite DR processes of a He-like ground-state ion, through the $1s2l2l'$ and $1s2l3l'$ doubly-excited, autoionizing states, can be represented by the following sequence of elementary transitions:

$$1s^2 + e^- \rightarrow 1s2ln'l' \quad (n'=2,3), \tag{18}$$

$$1s2ln'l' \quad (n'=2,3) \rightarrow 1s^2 2l + \hbar\omega_1, \tag{19a}$$

or

TABLE II. Resonances in the cross section for DR of He-like Fe^{24+} through the Li-like $1s2l2l'$ doubly-excited, autoionizing complex. The DR resonance transitions are labeled using the notation introduced by Gabriel [24]. E_{id} is the resonance energy. S_{idf} is the lowest-order resonance-transition strength, defined as an integration over the resonance profile by Eq. (13), for which the interference contribution vanishes and the RR contribution has been omitted. Where available, the corresponding experimental values (which are indicated by Expt.) measured in EBIT [22] are given for comparison with the calculated values (which are indicated by Calc.). Numbers in square brackets indicate powers of ten.

Transition	E_{id} (eV) Calc.	E_{id} (eV) Expt. [22]	S_{idf} (eV cm^2) Calc.	S_{idf} (eV cm^2) Expt. [22]
o	4554.5	4553.4	8.52[−21]	7.06[−21]
p	4554.5	4553.4	8.12[−21]	7.35[−21]
v	4565.4	4566.3	1.54[−22]	
u	4570.3	4570.1	1.31[−21]	
r	4606.6	4604.9	3.87[−20]	5.03[−20]
q	4616.7	4615.3	1.02[−21]	
h	4623.6	4624.6	2.56[−24]	
i	4623.6	4624.6	2.22[−22]	
t	4630.8	4631.2	5.63[−20]	
f	4631.5	4632.9	2.46[−21]	
g	4631.5	4632.9	3.87[−23]	
s	4633.8	4633.2	1.05[−20]	
e	4639.0	4639.0	3.78[−20]	3.90[−20]
k	4657.5	4658.1	1.84[−19]	
l	4657.5	4658.1	1.72[−20]	
c	4659.7	4658.6	2.25[−22]	
d	4659.7	4658.6	7.72[−22]	
j	4664.6	4664.1	3.36[−19]	
a	4677.5	4677.0	6.24[−20]	
b	4677.5	4677.0	1.22[−21]	
m	4697.2	4697.7	2.37[−20]	2.24[−20]
n	4697.2	4697.7	9.63[−22]	

$$1s2ln'l' \quad (n'=2,3) \rightarrow 1s^2n'l' + \hbar\omega_2 . \tag{19b}$$

It should be noted that the radiative stabilizations in Eqs. (19a) and (19b) may terminate on excited states that can undergo further decay by subsequent radiative transitions, giving rise to radiative cascades.

In the present investigation, the HULLAC code [23] has been adapted to provide the partial-wave radiative-emission and autoionization amplitudes, including the required quantum-mechanical phases. In Fig. 1, the calculated total PR cross section $\sigma_i^{PR}(\varepsilon)$ for He-like Ar in the ground state is presented as a function of the incident-electron energy ε, in the energy region of the Li-like $1s2l2l'$ doubly-excited, autoionizing resonances. Figure 2 shows the results of a similar calculation for He-like Fe. These results for the total PR cross section $\sigma_i^{PR}(\varepsilon)$ have been obtained by taking into account the three distinct contributions, corresponding to the RR, DR, and the interference components, as indicated by Eq. (4). The contributions of the entire set of $1s2l2l'$ doubly-excited, autoionizing states *d* have been included, as well as the corresponding set of singly-excited, bound states *f* that can be reached by electric-dipole-allowed radiative decays:

$$\sigma_i^{PR}(\varepsilon) = \sum_f \sigma_{if}^{RR}(\varepsilon) + \sum_{d,f} [\sigma_{idf}^{DR}(\varepsilon) + \sigma_{idf}^{int}(\varepsilon)]. \tag{20}$$

The total PR cross sections in Figs. 1 and 2 exhibit the DR-resonance peaks superimposed on the nonresonant RR continuum. Some of the resonance features show asymmetrical profiles, which are due to the effect of the quantum interference between the RR-continuum and the DR-resonance components. In these figures, the logarithmic scales tend to accentuate this asymmetry. For the designation of the DR-resonance features (dielectronic-satellite lines) that are associated with the individual radiative transitions from the $1s2l2l'$ doubly-excited, autoionizing states, we have adopted the familiar notation convention involving lower-case letters, which was originally introduced by Gabriel [24]. Since the sums over the final, bound states *f* are included in the definition of the electron-energy-dependent cross section given by Eq. (20), some of these spectral features are the result of two alternative radiative-decay channels [corresponding to the two distinct elementary transitions (19a) and (19b)] originating from an individual doubly-excited, autoionizing state *d*. Accordingly, these DR-resonance features are labeled by two different lower-case letters. In the emitted

x-ray spectrum, the two distinct radiative-decay channels will obviously give rise to two separate dielectronic-satellite features, which may be individually resolvable.

It is important to note that the resonance-transition strength S_{idf} defined by Eq. (13), which we consider to be the most experimentally accessible intensity measure for an individual DR-resonance transition $i \rightarrow d \rightarrow f$, is determined by performing an integration of the total energy-dependent PR cross section over the energy profile of the DR resonance. The dominant DR resonances, i.e., those with high S_{idf} values, are found to provide the primary contribution to the total PR rates and also to give rise to the most prominent DR-satellite lines. Consequently, the more relevant physical DR-resonance property in Figs. 1 and 2 corresponds to the area under the cross-section profile rather than the maximum value. Furthermore, a consideration of only the maximum values of the DR-resonance profiles in Figs. 1 and 2 can lead to incorrect interpretations. Specifically, the maximum value of the energy-normalized Lorentzian function is proportional to the reciprocal of its autoionizing-level width $\Gamma(d)$, which is defined by Eq. (10). This implies that the relatively weak DR-resonance transitions (with low S_{idf} values) usually have very narrow cross-section profiles with large maximum values. In EBIT experiments, S_{idf} is the quantity that is most directly measured, whereas the natural-width profile of the DR-resonance transition is not easily observed, due to the much broader electron-beam energy distribution.

In order to provide a more meaningful assessment of the relative importance of the DR resonances, beyond the information that can be obtained graphically, the entire set of the $1s2l2l'$ DR resonance-transition strengths that we have calculated in lowest-order perturbation theory is listed in Tables I and II, for Ar and for Fe, respectively. For the Fe case (Table II), the calculated DR data are compared with the measured results of Beiersdorfer *et al.* [22]. It can be seen that the calculated energy values are in excellent agreement with the experimental results, within 0.4%. For the DR resonance-transition strengths, single-channel experimental results are available for five resonance transitions, which are given in the last column of Table II. The uncertainty in these experimental S_{idf} values has been estimated [22] to be within 20%. It can be seen that all of the calculated values, except in the case of the DR-satellite feature *r*, are within this uncertainty range.

In the lowest-order perturbation-theory approximation adopted in the present investigation, the quantum-interference component of the PR cross section provides a vanishing contribution to the DR resonance-transition strength. This is a consequence of the completely asymmetric electron-energy dependence centered at the resonance level, which leads to a vanishing contribution when integrated over the resonance-energy profile. In order to provide a more accurate evaluation of the quantum-interference cross section, which would predict nonvanishing contributions to the DR resonance-transition strengths, it will obviously be necessary to retain higher-order terms in the perturbation-theory expansions. We emphasize that the higher-order terms have been neglected in the present investigation. However, the most pronounced spectral characteristic of the quantum-interference cross section, which is the asymmetric cross-section profile, can be realistically described and systematically evaluated within the framework of the lowest-order approximation adopted in our present calculations.

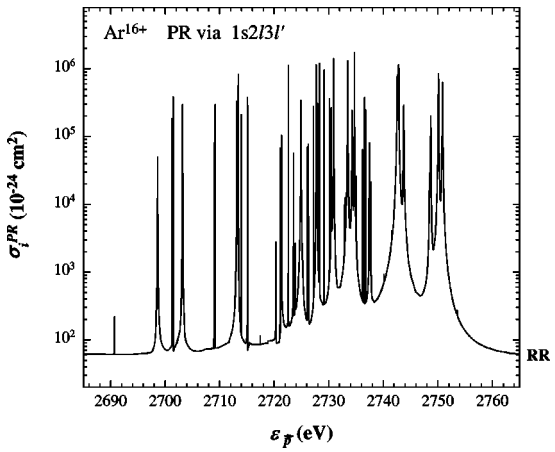

FIG. 3. Total cross section for PR of He-like Ar^{16+} for incident-electron energies in the vicinity of the Li-like $1s2l3l'$ doubly-excited, autoionizing complex, as a function of the incident-electron energy. The continuum contribution to the total PR cross section corresponds to the unperturbed RR component.

In the investigation of higher-lying DR resonances, we have calculated the total PR cross sections for ground-state He-like Ar and Fe ions, for incident-electron energies in the vicinity of the $1s2l3l'$ autoionizing-configuration complex of the corresponding Li-like ions. The results are shown in Figs. 3 and 4, for Ar and Fe, respectively. We find that the $1s2l3l'$ complex gives rise to numerous DR-resonance features, which are substantially overlapping in most cases. Dominant, isolated-resonance features with possibly detectable asymmetric profiles are not easily identifiable in this complex. A few relatively weak DR-resonance features in

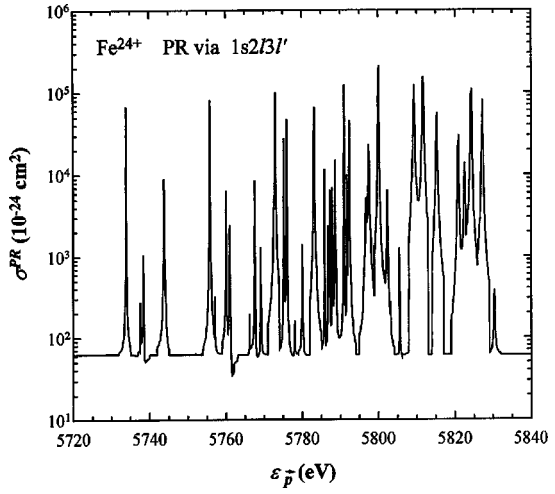

FIG. 4. Total cross section for PR of He-like Fe^{24+} for incident-electron energies in the vicinity of the Li-like $1s2l3l'$ doubly-excited, autoionizing complex, as a function of the incident-electron energy. The continuum contribution to the total PR cross section corresponds to the unperturbed RR component.

this complex (with $S_{idf} < 10^{-25}$ eV cm^2) are found to exhibit very strong asymmetries (for which $R^{int} > 100$). However, these DR-resonance features tend to lie very close to, and therefore merge with, the more prominent DR resonances.

The isolated-resonance approximation, which has been employed in the present investigation, may not provide a sufficiently accurate spectral description for the individual DR-resonance line shapes in the region of the numerous close-lying autoionizing levels corresponding to the $1s2l3l'$ complex. However, the isolated-resonant approximation may be adequate for an estimation of the total PR rates obtained by the summation over entire sets of resonance transitions, as discussed by Pindzola *et al.* [12]. In order to properly treat interactions among autoionizing resonances and radiative transitions among autoionizing states, the density-matrix approach proposed by Jacobs *et al.* [20] might provide a more appropriate framework. Using the asymmetry parameter defined by Eq. (17), an attempt is made in the next section to obtain a qualitative understanding of the spectral behavior that might be expected from the lowest-order quantum-interference effect for high-n' configurations.

In Table III, we present the cross-section asymmetry parameters that have been calculated for the $1s2l2l'$ resonances in the PR of He-like Ar and Fe. From these results, we deduce that the most asymmetric $1s2l2l'$ resonances correspond to the satellite features *l* of Ar and *q* of Fe. The results for the various contributions to the PR cross section are shown as functions of the incident-electron energy in Figs. 5 and 6, for the *l* feature of Ar and the *q* feature of Fe, respectively. From the results presented in Tables I and II, it can be seen that these satellite features correspond to relatively weak DR-resonance transitions. In the next section, we attempt to provide an explanation for the occurrence of the prominent asymmetries associated with relatively weak DR-resonance transitions. We also indicate how the ratio defined in Eq. (17) can be used to qualitatively investigate the general dependencies of the quantum-interference effect on the ion charge *q* and on the principal quantum number n' of the outer electron in the autoionizing state.

TABLE III. The parameter R^{int}, defined by Eq. (17), which reflects the degree of asymmetry in the total PR cross-section profile due to quantum interference between RR and DR, evaluated for recombination of He-like Ar^{16+} and Fe^{24+} through the Li-like $1s2l2l'$ doubly-excited, autoionizing complex. The DR resonance transitions are labeled using the notation introduced by Gabriel [24]. The most asymmetric resonance transition for each ion is indicated in boldface. Numbers in square brackets indicate powers of ten.

	R^{int}	
Transition	Ar^{16+}	Fe^{24+}
a	5.61[−3]	8.86[−3]
b	4.62[−2]	1.49[−1]
c	9.14[−2]	1.33[−1]
d	3.99[−2]	4.81[−2]
e	7.64[−3]	9.68[−3]
f	2.65[−3]	5.18[−3]
g	5.14[−2]	9.69[−2]
h	3.87[−2]	1.93[−1]
i	5.84[−3]	1.40[−2]
j	7.46[−3]	9.71[−3]
k	6.64[−3]	1.04[−2]
l	**5.51[−1]**	1.45[−2]
m	3.65[−3]	8.16[−3]
n	5.39[−3]	2.72[−2]
o	1.12[−2]	1.06[−2]
p	9.82[−3]	7.33[−3]
q	2.36[−2]	**2.09[−1]**
r	1.21[−2]	2.00[−2]
s	1.90[−2]	3.23[−2]
t	1.16[−2]	1.48[−2]
u	1.20[−2]	3.11[−2]
v	1.01[−2]	3.38[−2]

V. DISCUSSION AND SCALING OF THE QUANTUM-INTERFERENCE EFFECT

It should be possible to identify significant quantum-interference effects by means of systematic calculations for a representative variety of DR-resonance transitions in many ions, similar to the calculations of Pindzola *et al.* [12]. It would be useful to include evaluations of the ratio R^{int}, defined by Eq. (17), for the various arrays of DR-resonance transitions. Using the ratio R^{int}, we present a preliminary qualitative investigation of the variation of the quantum-interference effect with the ion charge *q*, and also with the principal quantum number n' of the outer electron in the doubly-excited, autoionizing state.

From the reciprocal relationship between the DR resonance-transitions strengths in Tables I and II and the R^{int} values presented in Table III, the largest quantum-interference effects are predicted for the weakest DR-resonance transitions. A qualitative understanding of this result is provided by means of a scaling analysis. The symbols *A* and A^a are used to represent the radiative decay and the autoionization rates, respectively, and the level designations are omitted. For the extreme case where $A^a \gg A$ (which pertains especially to low-charged ions), the DR resonance-transition strength *S*, defined by Eq. (13), and the DR cross section σ^{DR} scale linearly with *A*. However, the ratio R^{int} is found to scale as $(A^a/A)^{1/2}$, which tends to have a smaller value for the more intense radiative transitions. In the other extreme case where $A \gg A^a$ (which corresponds primarily to highly-charged ions), $S \sim A^a$ and $R^{int} \sim (A/A^a)^{1/2}$.

For the case of near equality in which $A \cong A^a$ and $S \sim A$ (which corresponds particularly to intermediately-charged ions), we predict that $R^{int} \sim (A)^0$ (i.e., independent of *A*). Consequently, for the intermediately-charged ions the effect of the quantum interference is expected to be approximately the same for both the dominant and the weak DR-resonance transitions. One might predict that the intermediately-charged ions would feature dominant DR-resonance transitions for which the quantum-interference effect is also strong. However, it is shown below that, in the intermediately-charged regime, the quantum-interference ef-

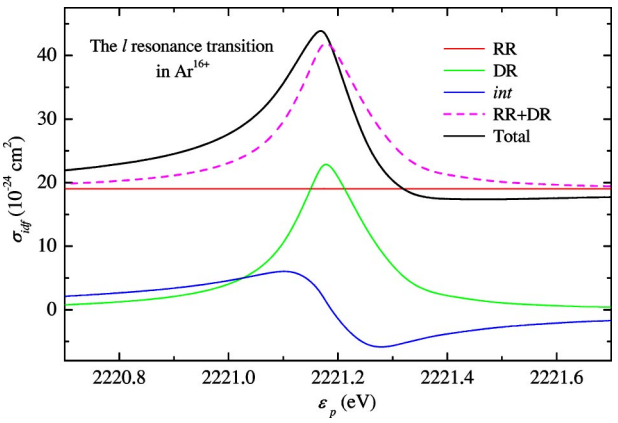

FIG. 5. (Color online) The cross section for PR of He-like Ar^{16+} in the vicinity of the DR-resonance transition *l*. The total PR cross section (σ^{PR}) is represented by a black line. The direct, nonresonant RR cross section (σ^{RR}) is indicated by a red line, the two-step, resonant DR cross section (σ^{DR}) is indicated by a green line, the interference contribution (σ^{int}) is indicated by a blue line, and the sum of the RR and DR contributions is indicated by a dotted red line.

fect is expected to be weaker than for the two extreme cases (discussed above) corresponding to very low- or very highly-charged ions.

To investigate the behavior of the ratio R^{int} as a function of the ion charge q, we employ a hydrogenic-scaling analysis. A similar analysis, which should be most appropriate for highly-charged species, has been previously used by Hahn [25] for the DR-rate coefficients. The differences between the energies of atomic states with different principal quantum numbers (i.e., $\Delta n \geqslant 1$), as well as the corresponding electron and photon energies ε and $\hbar\omega$, scale as q^2. The incident-electron linear momentum p scales as q, and the energy-normalization electron-continuum wave functions ψ_c scale as $p^{1/2} \sim q^{1/2}$. The bound-state wave functions ψ_b scale as $q^{3/2}$. The electric-dipole interaction between the atomic system and the electromagnetic field scales as $r \sim q^{-1}$, while the electron-electron electrostatic interaction scales as $1/r \sim q$.

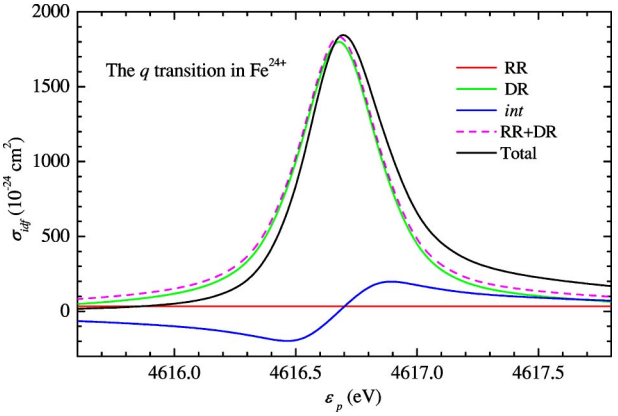

FIG. 6. (Color online) The cross section for PR of He-like Fe^{24+} in the vicinity of the DR-resonance transition *q*. The total PR cross section (σ^{PR}) is represented by a black line. The direct, nonresonant RR cross section (σ^{RR}) is indicated by a red line, the two-step, resonant DR cross section (σ^{DR}) is indicated by a green line, the interference contribution (σ^{int}) is indicated by a blue line, and the sum of the RR and DR contributions is indicated by a dotted red line.

The q scaling of Q_{idf} can be investigated by considering the various matrix elements in the definition given by Eq. (15). For the $\Delta n \geqslant 1$ bound-bound radiative transitions, the electric-dipole-interaction matrix element scales as follows:

$$\langle \gamma_f J_f \| \vec{D} \| \gamma_d J_d \rangle \sim \psi_b r \psi_b d^3 r \sim q^{3/2} q^{-1} q^{3/2} q^{-3} = q^{-1}. \tag{21}$$

Consequently, the Einstein A coefficient given by Eq. (11) has the well-known q^4 scaling. The matrix element for autoionization scales as follows:

$$\langle \gamma_i J_i, \varepsilon\kappa; J \| H_{es} \| \gamma_d J_d \rangle \sim \psi_b \psi_c \frac{1}{r} \psi_b \psi_b d^3 r_1 d^3 r_2 \sim q^{3/2} q^{1/2} q q^{3/2} q^{3/2} q^{-3} q^{-3} = q^0. \tag{22}$$

This gives rise to the well-known charge independence of the nonrelativistic autoionization rate. The free-bound electric-dipole-transition (RR) matrix element scales according to the relationship

$$\langle \gamma_f J_f \| \vec{D} \| \gamma_i J_i, \varepsilon\kappa; J \rangle \sim \psi_b r \psi_c d^3 r \sim q^{3/2} q^{-1} q^{1/2} q^{-3} = q^{-2}. \tag{23}$$

Consequently, the RR cross section given by Eq. (6) scales as q^0 (i.e., independent of q). Taking into account the scaling relationships given by Eqs. (21), (22), and (23), we obtain the result

$$\frac{1}{Q_{idf}} \sim \frac{\langle \gamma_f J_f \| \vec{D} \| \gamma_i J_i, \varepsilon\kappa; J \rangle \langle \gamma_i J_i, \varepsilon\kappa; J \| H_{es} \| \gamma_d J_d \rangle}{\langle \gamma_f J_f \| \vec{D} \| \gamma_d J_d \rangle} \sim q^{-2} q^0 / q^{-1} = q^{-1}. \tag{24}$$

To investigate the q scaling of the ratio R^{int} defined by Eq. (17), it is again necessary to consider two different cases. For $A^a \gg A$, $\Gamma(d) \sim A^a \sim q^0$ and $R^{int} \sim q^{-1}$. Accordingly, for low-q ions, the asymmetry is expected to *decrease* with increasing ion charge. In the other case, for $A \gg A^a$, $\Gamma(d) \sim A \sim q^4$ and $R^{int} \sim q^3$. Consequently, for high-q ions the asymmetry is expected to rapidly *increase* with increasing ion charge. For the general case, including the intermediate-q regime, $\Gamma(d) \sim (aq^0 + bq^4)$ and consequently $R^{int} \sim (aq^{-1} + bq^3)$, where a and b are constants (usually $a \gg b$). In summary, the asymmetry of the total PR cross-section profile is predicted to be prominent for close-to-neutral ions and significant for very highly-charged ions. However, in the intermediate-charge regime, the asymmetry is anticipated to be the least prominent.

The q-scaling analysis presented above may provide a qualitative understanding for the pronounced asymmetrical profiles that have been detected for U^{88+} [10] and for Sc^{3+} [11]. This analysis is in agreement with the conclusion,

reached in an extensive investigation by Pindzola *et al.* [12], that the largest interference effects are generally expected to be found in the extreme cases of very highly-charged ions and neutrals. For the majority of significantly intense DR-resonance transitions in intermediately-charged ions, including those considered in the present investigation, only a weak degree of asymmetry is found. It should be pointed out that the experimental results obtained for the PR of Sc^{3+} [11] exhibit a more complex spectral variation than that predicted using the simplified hydrogenic-scaling analysis. This is due to configuration mixing involving the $3p$ and $4s$ states, which alters the $(\Delta n=0)$ $3p-3d$ and the $(\Delta n=1)$ $3p-4s$ transition rates. The hydrogenic-scaling analysis is obviously invalid for $\Delta n=0$ transitions.

We now investigate the scaling of the ratio R^{int}, which is defined by Eq. (17), for high-n' configurations, where n' is the principal quantum number of the outer electron in the doubly-excited, autoionizing state. The wave functions representing the doubly-excited, autoionizing states are assumed to scale as $(n')^{-3/2}$. The relevant RR transitions do not involve the high-n' levels and their rates are therefore independent of n'. However, the high-n' radiative-decay and autoionization rates A and A^a both scale as $(n')^{-3}$. For the case $A^a \gg A$, we obtain $R^{int} \sim (A^a/A)^{1/2} \sim (n')^0$. For the other case $A \gg A^a$, we find that $R^{int} \sim (A/A^a)^{1/2}$, which also scales as $(n')^0$. A different scaling of the rates is found in the case of a radiative stabilization of the lower excited n electron, e.g., $1s2ln'l' \rightarrow 1s^2n'l'$. Since the autoionization process $1s2ln'l' \rightarrow 1s^2$ still involves the n' electron, A^a retains the $(n')^{-3}$ scaling, while A now scales as $(n')^0$. For these decay channels we obtain, for the extreme case $A^a \gg A$, $R^{int} \sim (A^a/A)^{1/2} \sim (n')^{-3/2}$. For the other extreme case $A \gg A^a$, we find that $R^{int} \sim (A/A^a)^{1/2} \sim (n')^{3/2}$. We point out that, for the radiative-decay processes that do not involve the n' electron, the condition $A \gg A^a$ may occur not only for high-q ions but also for low-q ions in levels with high-n' values. This is a result of the rapid decrease in A^a with increasing n' and of A being independent of n'. In the intermediate regime, as in the general case, we find that $\Gamma(d) \sim a(n')^0 + b(n')^{-3}$ and consequently $R^{int} \sim a(n')^{3/2} + b(n')^{-3/2}$, where a and b are constants.

As a result of our analysis, we find that, in DR processes that involve the radiative decay of the intermediate autoionizing state through a transition of the highly-excited n' electron, the degree of asymmetry of the total PR cross section, as reflected by the ratio R^{int}, is not expected to be strongly dependent on n'. On the other hand, in DR processes that do not actively involve the radiative decay of the n' electron, the asymmetry of the total PR cross section is predicted to at first decrease with increasing n', but eventually to increase with increasing n'. It should be emphasized that our conclusions pertaining to the n' scaling of the quantum-interference effect are expected to be valid provided that the isolated-resonance approximation, which is assumed in the derivation of Eq. (17), continues to provide an adequate representation for the high-n' levels.

VI. CONCLUSIONS

A unified description of radiative and dielectronic recombination, which is based on a projection-operator and resolvent-operator formulation, has been applied to compute the total photorecombination (PR) cross sections of He-like argon and iron ions for incident-electron energies in the vicinity of the $1s2l2l'$ and $1s2l3l'$ autoionizing-configuration complexes. This theoretical description of PR is based on a fundamental quantum-mechanical foundation, and it is expected to be rigorously valid at low plasma densities. In order to facilitate the calculations, a perturbation-theory expansion of the transition operator has been used. If only the lowest-order contributions in the perturbation-theory expansion are retained, the familiar expressions for the direct (nonresonant) radiative-recombination and two-step (resonant) dielectronic-recombination cross sections are recovered. In addition, the lowest-order quantum-interference cross section is obtained, in terms of the basic, unperturbed (lowest-order) transition amplitudes that are conventionally associated with direct radiative recombination, autoionization, and radiative emission. These unperturbed (lowest-order) transition amplitudes are calculated by means of the modified HULLAC code, which has been especially adapted for this investigation.

Results for the total PR cross sections of He-like argon and iron ions are presented for incident-electron energies in the vicinity of the $1s2l2l'$ and $1s2l3l'$ autoionizing-configuration complexes. For certain weak satellite features, significant effects of quantum interference are revealed in the form of radiatively modified, asymmetric (Fano-type) cross-section profiles. In lowest-order perturbation theory, the interference cross sections are predicted to be entirely asymmetric with respect to the resonance positions and, consequently, cannot contribute to the resonance-transition strengths obtained by integration over the resonance profiles. For some of these weak transitions, the highly asymmetric cross-section profiles could be observable with the individual spectral resolution of the distinct x-ray emission lines associated with the different radiative-decay channels. Because of the sub-eV natural width of the DR-resonance features, the measurement of the detailed spectral profiles presents a substantial challenge with the resolution of current electron beam experiments. We anticipate, however, that the detailed DR-resonance profiles will be resolved in future experiments.

There are several directions in which the present investigation should be extended. In order to obtain more detailed representations of the DR-resonance profiles, and in particular the nonvanishing interference contributions to the resonance-transition strengths, it will be necessary to derive and evaluate the higher-order perturbation-theory contributions to the low-density PR cross section. In order to pursue the search for significant and experimentally observable interference effects, DR-satellite transitions in more complex atomic systems should be investigated. This investigation could be facilitated by the scaling analysis presented in Sec. V for the charge and the principal-quantum-number dependencies of the asymmetry parameter defined by Eq. (17). The angular distribution and polarization of the emitted satellite radiation should also be evaluated to broaden the search for more pronounced quantum-interference phenomena, whose effects could be more readily observable in electron-beam

experiments. Finally, the low-density theory should be extended to incorporate environmental collisional and radiative decoherence and relaxation processes, which are expected to play important kinetic and spectral roles at sufficiently high plasma densities and/or at sufficiently high radiation-field intensities. By means of a reduced-density-matrix formulation [20], the collisional and radiative decoherence and relaxation processes can be treated on an equal footing and in a self-consistent manner with the quantum-coherent autoionization and radiative-emission processes.

ACKNOWLEDGMENTS

E.B. acknowledges the support of the Yigal Alon Foundation by the Israeli Counsel for Higher Education. The research work of V.L.J. has been supported by the U.S. Department of Energy and by the Office of Naval Research. The research work of S.L.H. has been supported by the National Science Foundation through Grant No. PHY-0099381 to Calvin College.

[1] G. Alber, J. Cooper, and A. R. P. Rau, Phys. Rev. A **30**, 2845 (1984).
[2] V. L. Jacobs, Phys. Rev. A **31**, 383 (1985).
[3] K. J. LaGattuta, Phys. Rev. A **36**, 4662 (1987); **38**, 1820 (1988).
[4] V. L. Jacobs, J. Cooper, and S. L. Haan, Phys. Rev. A **36**, 1093 (1987).
[5] N. R. Badnell and M. S. Pindzola, Phys. Rev. A **45**, 2820 (1992).
[6] M. S. Pindzola, F. Robicheaux, N. R. Badnell, M. H. Chen, and M. Zimmermann, Phys. Rev. A **52**, 420 (1995).
[7] T. W. Gorczyca, M. S. Pindzola, F. Robicheaux, and N. R. Badnell, Phys. Rev. A **56**, 4742 (1997).
[8] D. M. Mitnik, M. S. Pindzola, and N. R. Badnell, Phys. Rev. A **59**, 3592 (1999).
[9] E. Behar, V. L. Jacobs, A. Bar-Shalom, J. Oreg, and S. L. Haan, Phys. Rev. A **62**, 030501(R) (2000).
[10] D. A. Knapp, P. Beiersdorfer, M. H. Chen, J. H. Scofield, and D. Schneider, Phys. Rev. Lett. **74**, 54 (1995).
[11] S. Schippers, S. Kieslich, A. Müller, G. Gwinner, M. Schnell, A. Wolf, A. Covington, M. E. Bannister, and L. B. Zhao, Phys. Rev. A **65**, 042723 (2002).
[12] M. Pindzola, N. R. Badnell, and D. C. Griffin, Phys. Rev. A **46**, 5725 (1992).
[13] F. Robicheaux, T. W. Gorczyca, M. S. Pindzola, and N. R. Badnell, Phys. Rev. A **52**, 1319 (1995).
[14] T. W. Gorczyca, F. Robicheaux, M. S. Pindzola, and N. R. Badnell, Phys. Rev. A **54**, 2107 (1996).
[15] K. A. Berrington, W. B. Eissner, and P. H. Norrington, Comput. Phys. Commun. **92**, 290 (1995).
[16] T. W. Gorczyca, N. R. Badnell, and D. W. Savin, Phys. Rev. A **65**, 062707 (2002).
[17] T. W. Gorczyca and N. R. Badnell, Phys. Rev. Lett. **79**, 2783 (1997).
[18] S. L. Haan and V. L. Jacobs, Phys. Rev. A **40**, 80 (1989).
[19] M. Zimmermann, N. Grün, and W. Scheid, J. Phys. B **30**, 5259 (1997).
[20] V. L. Jacobs, J. Cooper, and S. L. Haan, Phys. Rev. A **50**, 3005 (1994).
[21] V. L. Jacobs, J. E. Rogerson, M. H. Chen, and R. D. Cowan, Phys. Rev. A **32**, 3382 (1985).
[22] P. Beiersdorfer, T. W. Phillips, K. L. Wong, R. E. Marrs, and D. A. Vogel, Phys. Rev. A **46**, 3812 (1992).
[23] A. Bar-Shalom, M. Klapisch, and J. Oreg, J. Quant. Spectrosc. Radiat. Transf. **71**, 169 (2001).
[24] A. H. Gabriel, Mon. Not. R. Astron. Soc. **160**, 99 (1972).
[25] Y. Hahn, Adv. At. Mol. Phys. **21**, 123 (1985), p. 186 therein.